

Effect of N^+ irradiation on the microstructural and magnetic properties of Co/Pd multilayers

A.M. Testa^{1,a}, D. Fiorani¹, M.S. Martin-Gonzalez², F. Briones², J. Montserrat³, and H. Rohrmann⁴

¹ ISM – CNR, Area della Ricerca di Roma, P.B. 10, 00016 Monterotondo Stazione, Rome, Italy

² Instituto de Microelectrónica de Madrid, IMM (CNM-CSIC) C/Isaac Newton, 8 (PTM) 28760 - Tres Cantos, Madrid, Spain

³ Institut de Microelectrònica Barcelona, Campus Universitat Autònoma Barcelona, 08193, Bellaterra, Spain

⁴ UNAXIS Data Storage, 9496 Balzers, Liechtenstein

Received: 14 November 2006 / Accepted: 23 March 2007

Published online: 30 May 2007 – © EDP Sciences

Abstract. Microstructural and magnetic properties of $^{14}N^+$ irradiated Co/Pd multilayers, deposited on ultra-flat large (2.5 in) glass substrates by a special hard disk industrial manufacturing system, are discussed. Upon irradiation with $^{14}N^+$ ions at different energies (20–30 keV) and doses (10^{14} – 10^{15} ions/cm²), both the coercive and nucleation fields were found to change with respect to as deposited multilayer. Results indicate that the irradiation process leads to a lowering of the magnetic anisotropy due to the induced disorder and degradation of the interface quality: for an energy of 30 keV, at an irradiation level of 10^{15} ions/cm², H_c reduces from $H_c \approx 5.4$ kOe for the as deposited multilayer down to 300 Oe, being the easy axis still perpendicular to the multilayer plane; at the highest dose (10^{16} ions/cm²), the coercivity vanishes and the perpendicular anisotropy is suppressed.

PACS. 75.50.Ss Magnetic recording materials – 75.70.Cn Magnetic properties of interfaces (multilayers, superlattices, heterostructures) – 75.60.Jk Magnetization reversal mechanisms

1 Introduction

Ion irradiation has the potential to tailor the magnetic properties of ultrathin magnetic films and multilayers (e.g. magnetic anisotropy, exchange coupling) of materials systems relevant for technological applications [1], e.g. magnetorecording media.

In multilayers the tailoring of magnetic properties by ion irradiation involves changes in the microstructural properties, interface sharpness, chemical composition of the films and degree of intermixing and of chemical alloying at the interface. A prerequisite for the tuning of magnetic properties is the use of low energy light ions, which can induce short range atomic displacements.

Co/Pd and Co/Pt multilayers with small Co thickness (i.e. ≤ 8 Å) [2] are known to exhibit a perpendicular anisotropy, induced by strong interface effects [3] able to overcome the macroscopic shape anisotropy. This, together with high coercivity and high remanent squareness [4,5], makes such superlattices promising candidates for ultrahigh-density perpendicular magnetorecording media [6]. It has been demonstrated that the use of controlled intermixing by low energy (30 keV) He^+ [7–9] irradiation in Co/Pt ultrathin layers provides a control of the magnetic properties. Indeed, in Pt/Co (5 Å)/Pt layers, the

coercivity was reduced in a controlled way by adjusting the irradiation fluence, preserving the squareness of hysteresis loops. It has been also shown that planar patterned magnetic nanostructures can be realized through nanolithographically made masks [10,11]. This has opened new perspectives in the production of patterned recording media, where surface planarity is crucial. In this context, we have investigated the evolution, upon low energy N^+ irradiation, of structural and magnetic properties of Co/Pd multilayers, deposited on ultra-flat large (2.5 in) glass substrates by a special hard disk industrial manufacturing system.

2 Experimental

$[Co/Pd]_n$ multilayers were produced in a special hard disk commercial system (Unaxis, M12 Circulus) capable to fulfill actual hard disk production requirements (1000 disks/h; deposition time for the multilayer stack not exceeding 2.8 s). The system has ten individual double-sided process modules, a single module consisting of a deposition source with 3 concentric sputter targets (TriatronTM, Unaxis [6]; Kr sputtering pressure set at 37×10^{-6} bar (28 mTorr)). All changes of layer material, composition or thickness can be done by electrical switching only, providing the fast multilayer deposition: this led

^a e-mail: albertomaria.testa@ism.cnr.it

to reproducible conditions for fast (30 layers in less than 3 s) fabrication of high quality Co/Pd multilayers.

Amorphous Ti (20 nm thickness) and Pd (12 nm) seed layers, were pre-deposited on 2.5 in hard-disk HOYA glass substrates. The sublayer thickness of Co (Pd) was set at 0.2 (0.9) nm, with a number of 15 bilayers; the multilayer was covered by a 5 nm protective overcoat of diamond-like carbon.

The structure was studied by X-ray diffraction (XRD) and TEM. XRD was used to measure the lattice parameters; glancing incidence X-ray reflectometry (XRR) was used to measure the films thickness and to check possible variation upon implantation, using a PHILIPS X-PERT four-circle diffractometer. TEM investigation was performed in order to study the effect of microstructural characteristics on the magnetic properties. Selected area electron diffraction (SAD) was also used to gain information on crystallographic parameters and orientations of specific regions of the samples investigated. SAD is currently used to identify phases and grain textures in recording media. The experimental diffraction patterns were taken in $||$ -view at 0° tilting angle, at a camera length of 30 cm. Various SAD patterns were also taken at different tilting angles up to 50° to search for textured grains. $^{14}\text{N}^+$ ions implantation was carried out in an Eaton NV4206 equipment, with doses ranging from 10^{14} up to 2×10^{16} ions/cm² and ions energy set at 20–30 keV. The highest values were chosen so that the maximum damage is produced in the Co/Pd multilayers, according to computer simulation using the SRIM code [12] which uses the real stopping power of the different layers.

For Co/Pd multilayers, $^{14}\text{N}^+$ implantation behaves in the same way of a non reactive gas such as He [13], since no chemical bonding N-Co or N-Pd occurs and the unique effect of implantation is the induction of microstructural changes at Co/Pd interfaces. This is different for the case of Fe based films or multilayers where a chemical bonding Fe-N is detected [14].

Hysteresis loops were measured at room temperature by a home-made magneto-optical Kerr and commercial AGFM and vectorial VSM magnetometers.

3 Results and discussion

3.1 Microstructural and morphological properties

The SAD patterns were found to fit very well with the simulated CoPd fcc arc patterns. The lattice parameter of CoPd varies with the Pd concentration ($\text{Co}_{1-x}\text{Pd}_x$, $x = 0-1$, $a = 0.354-0.389$ nm). For calculations, the lattice parameter has been linearly interpolated. Figure 1 shows a typical SAD diffraction pattern taken in plane view (left panel), with measured and calculated diffraction patterns (right panel), showing the matching between ring radius and intensity of CoPd fcc (disordered) structure phase; the (hkl) -values are listed in Table 1. Texturing, as signaled by arcs instead of closed rings at high tilting angles in SAD patterns have not been found in all investigated samples. The presence of CoPd alloy was also

Table 1. list of (hkl) -values of the first ten radii [mm] of CoPd fcc with $d(hkl)$ -values [nm] and intensities (max vale: 1000), respectively.

Nr.	h	k	l	d_{hkl} [nm]	Radius [mm]	Intensity
1	1	1	1	0.2200	11.4	1000
2	0	0	2	0.1905	13.2	491
3	2	0	2	0.1347	18.6	320
4	1	1	3	1.1149	21.8	360
5	2	2	2	0.1100	22.8	102
6	0	0	4	0.0952	26.4	43
7	3	1	3	0.0874	28.7	118
8	2	0	4	0.0852	29.5	105
9	2	2	4	0.0778	32.3	69
10	3	3	3	0.0733	34.2	17

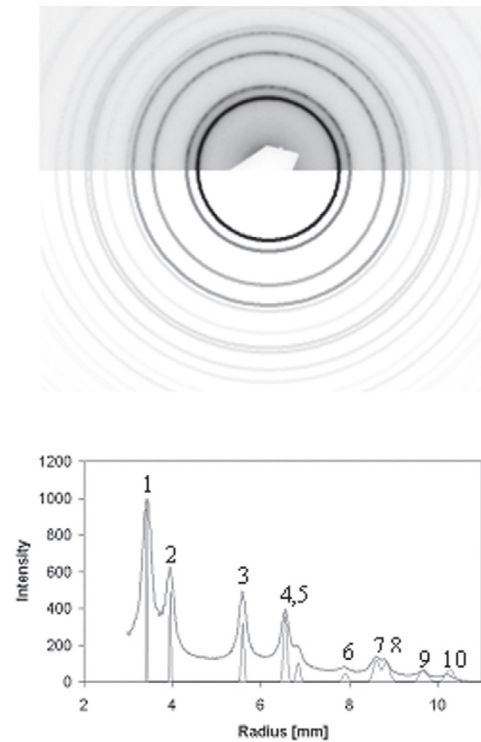


Fig. 1. Upper panel: typical SAD pattern (positive); lower panel: comparison between calculated and measured radii and intensities.

confirmed by XRD, where the (111) diffraction peak was identified.

In general, the magnetic decoupling of the grains strongly depends on the preparation conditions of the films, such as type and pressure of sputter gas. For instance, high Ar gas pressure has been reported to cause a large increase of H_c in $[\text{Co}/\text{Pd}]_n$ multilayers [15]. In our case, TEM investigations showed columnar grains (size ≈ 10 nm) surrounded by voids (Fig. 2). The roughness of the layers was found to increase layer by layer along the normal to the surface. Figure 2, left panel: such roughness leads to groove formation caused by shadowing effect [16]

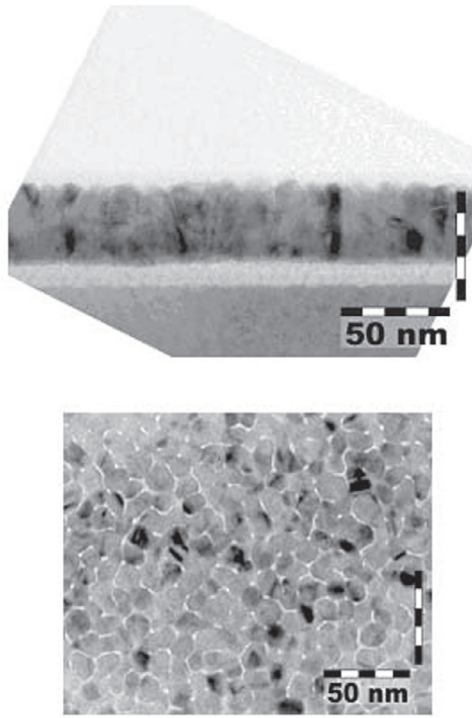


Fig. 2. TEM bright field micrographs: upper panel: cross sectional view; lower panel: plane view of the columnar growth showing voids formation.

(occurred at high gas pressure) which, in turn, leads to groove and void formation around magnetic grains, i.e. to a loss in film density. The presence of intercolumnar voids (Fig. 2, right panel) can thus lead to magnetic exchange decoupling (at least for the in plane direction).

Typical XRR spectra are shown in Figure 3 for the as deposited and irradiated multilayers: they show fringes at angular position in close agreement with the total metallic thickness of the film. The fringe frequency does not decrease on increasing the implantation dose until 10^{15} ions/cm², indicating that the implantation has a low effect on the total thickness of the samples. In other words, there are no sputtering effects for the doses and energies employed in this study and, hence, the total thickness of the film is unchanged after implantation for doses as high as 10^{15} ions/cm².

3.2 Magneto-optical properties and study of the magnetization processes

Magnetization measurements, performed on as prepared Co/Pd multilayers, applying the field perpendicular to the film plane, show a square hysteresis loop (Fig. 4, top panel) with perpendicular easy axis of the magnetization (along the normal to the film substrate), with coercivity

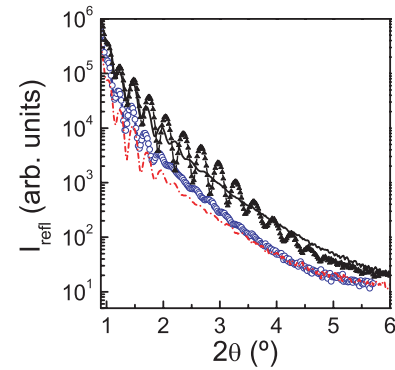


Fig. 3. Glancing angle X-ray diffraction of the as deposited (solid line) and irradiated multilayers: 10^{14} ions/cm² (open blue symbols); 10^{15} ions/cm² (dash-dot red line); 2×10^{16} ions/cm² (line with closed symbols).

$H_c = 5430$ Oe, an anisotropy field of 13 kOe (estimated from the hard axis magnetization loop, not shown) and negative nucleation field. The coercive field is within the values reported in the literature [17–19] where the spread of values is associated to the high sensitivity of the coercivity to process conditions such as sputter gas pressure, type and thickness of seed layer, Co and Pd sublayer thickness. Such a large interface anisotropy, overcoming the macroscopic shape anisotropy, is expected for a so small thickness (2 Å) the Co layers. The perfectly square hysteresis loop, with a negative nucleation field H_N almost equal to the H_c , would suggest that the reversal is governed by nucleation of a reversed region, with the weakest anisotropy, followed by rapid wall motion. However, the angular dependence of the zero remanence coercivity (i.e. remanent magnetization measured after saturation and application of a reverse magnetic field, Fig. 5) show a Stoner-Wolfarth like behavior, expected for coherent magnetization reversal. This can be the case if the nucleation field (which actually determines the observed angular dependence) is much larger than the wall propagation field. Moreover, the high value of the steepness at the coercivity ($\alpha = 4\pi(dM/dH) = 8$ G/Oe) [20] also indicates a collective reversal of magnetization due to the large intracolumnar exchange coupling and magnetic polarization of Pd regions induced by adjacent Co sublayers [21] (the ideal value of α for a loop shearing due to shape demagnetizing field is 1G/Oe). This is expected as the grain size is of the order of the Co-Pd exchange length (i.e. 17–24 nm [22]).

Upon irradiating with $^{14}\text{N}^+$ ions at different energies (20–30 keV) and doses (10^{14} – 10^{15} ions/cm²), both the coercive and nucleation fields were found to change with respect to the as deposited multilayer. Up to an irradiation level of 10^{15} ions/cm² (Fig. 4 middle panel) H_c reduces down to 307 Oe whereas the perpendicular easy axis is preserved (the remanent ratio (M_r/M_s) ≈ 1). The decrease of H_c is determined by microstructural changes (e.g. change of short range order around interface Co atoms, possible Co-Pd intermixing or/and partial Co-Pd alloying, stress relaxation at the interface and interface roughing) induced

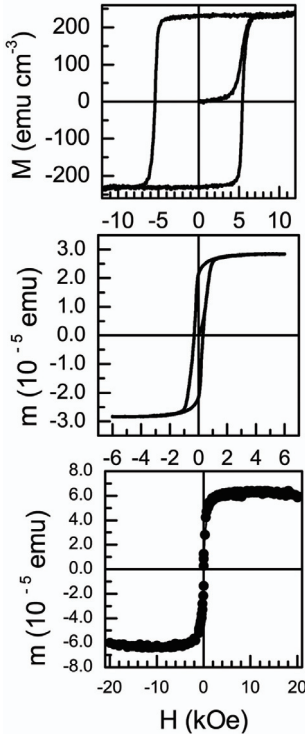


Fig. 4. Magnetization as function of external magnetic field (applied along the normal to the film substrate) for multilayers as deposited (top panel); irradiated at different ion doses and fixed energy (30 keV): 10^{15} (middle); 2×10^{16} ions/cm² (bottom).

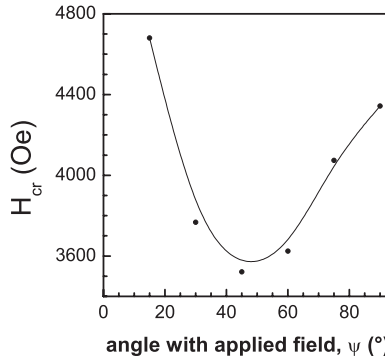


Fig. 5. Zero remanence coercivity as a function of the angle between applied field and film surface.

by the irradiation. This should result in a reduction of defects actually pinning the domain walls.

At the highest dose (10^{16} ion/cm², Fig. 4, bottom panel), the coercivity vanishes and the perpendicular anisotropy is suppressed, the easy axis moving from the out of plane to the in plane film direction. At larger doses the multilayer becomes even paramagnetic. Moreover, magnetization vs. field measurements (not shown) reveal a full paramagnetic behavior above 450 K, to be compared to the Curie temperature $T_c = 570$ K of the unirradiated CoPd multilayer [23]. A significative decrease of Curie temperature is an effect concomitant to the decrease of coercive field, as reported in the liter-

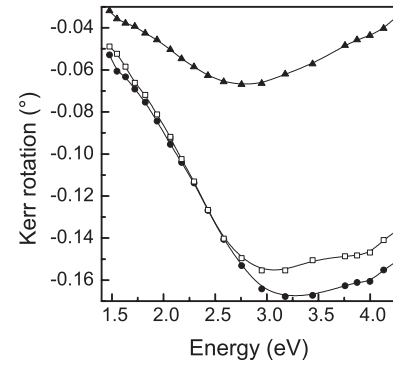


Fig. 6. Room temperature Polar Kerr spectra of unirradiated (closed circles) and irradiated (10^{15} : open squares; 2×10^{16} ions/cm²: closed triangles) multilayers.

ature [24]. The reduction of anisotropy induced by implantation makes thermal fluctuations more effective in destabilizing the long range ferromagnetic order: such a picture of a destabilized ferromagnetic LRO via a reduction of anisotropy is further supported by the room temperature Polar Kerr Spectra (Fig. 6), showing a drastic reduction of the Kerr rotation amplitude (which is proportional to M_s) in the sample irradiated at the highest dose (2×10^{16} ion/cm²).

Magnetization reversal processes and their dependence on the N^+ irradiation were further investigated by isothermal remanent magnetization (IRM) and remanence magnetization after demagnetization (DCD) measurements. The IRM curve, measured starting from the demagnetized state, applying a field and then measuring the remanence, charts the progress of the net remanent magnetization free of nucleation effects as the measurement start from a macroscopic zero magnetization state. The DCD remanence curve is measured by first saturating the sample in a positive applied field, applying a given reverse field and then measuring the magnetic moment at zero applied field. DCD remanence curves detect nucleation effects as the measurement starts from the saturated state. Differentiating the normalized remanence curves with respect to the applied field gives the irreversible susceptibility χ_{irr} which maps the energy barrier distribution for the process measured by the curve. Thus differentiating the IRM remanence curve gives the domain wall pinning energy barrier distribution whilst differentiating the DCD remanence curves leads, in the ideal case, to the domain nucleation energy barrier distribution, or more often, to a convolution of the domain nucleation and domain wall pinning energy barrier distributions. The irreversible susceptibility, χ_{irr} , is reported in Figure 7: the maxima are at fields corresponding to the center of the distribution of the switching fields. For the unirradiated multilayer, χ_{irr} shows a single peak at 5500 Oe (Fig. 7, top panel), irrespective of the initial state of the system (virgin or saturated for IRM and DCD measurements, respectively); for a dose of 10^{15} ions/cm² (Fig. 7, bottom panel), χ_{irr} from DCD has peaks in the low field region, $H_1 = 120$ Oe and $H_2 = 750$ Oe, overlapping that from IRM which displays a single peak at

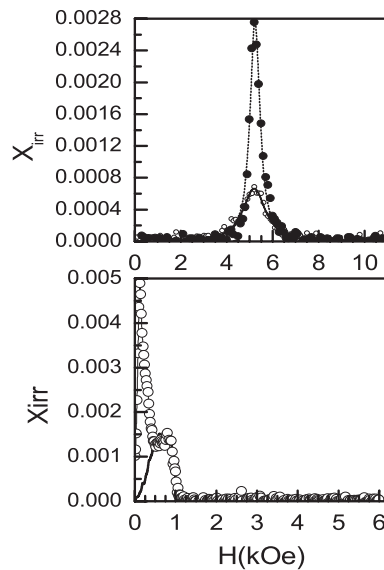


Fig. 7. Irreversible susceptibility for the unirradiated (top panel) (solid line: from IRM; dotted line and closed symbols: from DCD) and irradiated (dose of 10^{15} ions/cm²) samples: (bottom panel; solid line: from IRM; open symbols: from DCD).

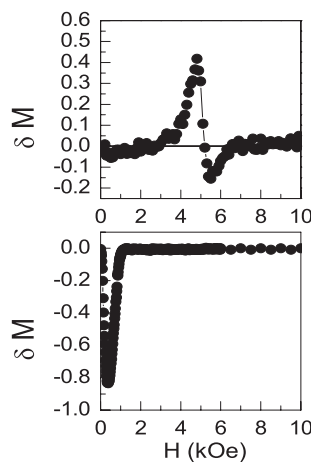


Fig. 8. δM plots for unirradiated (top panel) and irradiated (10^{15} ions/cm²; bottom panel) multilayers.

H_2 . Such shift of the switching field distribution to lower fields provides a further clear evidence of the reduction of anisotropy after N^+ irradiation.

IRM and DCD remanence curves can be combined to yield the so called modified Henkel plots [25] (δM), reported in Figure 8 for as deposited and irradiated multilayers. Positive $\delta M(H)$ plots indicate that the interactions encourage the magnetized state, as in exchange coupled granular systems; negative $\delta M(H)$ plots are exhibited by materials such as fine particle systems and particulate recording media, where the coupling is dipolar in nature.

Two maxima (positive and negative) are observed for the as deposited multilayer, indicating the coexistence of both exchange (intra-columnar) and dipolar (inter-columnar) type interactions, respectively: the positive

peak has a larger amplitude than the negative one, indicating the predominance of exchange interactions. After an irradiation at 10^{15} ions/cm², only one negative peak is observed, shifted to lower fields value: this indicates a strong weakening of intra-columnar exchange interactions with irradiation, well coherent with the decrease of anisotropy, as both rely to the interface quality microstructure, which is degraded by the irradiation. Coherently, the granular character of the multilayer is strongly enhanced, as shown by the increase of amplitude of the negative peak.

4 Summary and conclusions

We have investigated the effect of irradiation with ^{14}N ions of controlled energy and dose on the microstructural and magnetic properties of Co/Pd multilayers produced by a special hard disk industrial manufacturing system.

The results indicate that irradiation induces a decrease of coercivity likely associated to a reduction of defects actually pinning the domain walls. The perpendicular easy magnetization axis is preserved for an irradiation energy of 30 keV and dose of 10^{15} ions/cm². The decrease of coercivity is accompanied by a decrease of Curie temperature and an increase of the granular character of the multilayers. Irradiation does not induce significant modification of the film thickness and surface roughness. Such results indicate that the low energy irradiation through nanosized masks could be used to produce a regular magnetic contrast, i.e. an array of paramagnetic and hard regions, without affecting the film planarity. This approach could represent a promising efficient, rapid and low cost nanopatterning method for developing patterned recording media.

The EU HIDEMAR project (c No. G5RD-CT-2002-00731) is gratefully acknowledged for financial support. We would like also thanks to Prof. G. Armelles for help with the magneto-optical measurements. One of the authors (MSMG) would like to thank the Ramon y Cajal Program.

References

1. J. Fassbender, D. Ravelosona, Y. Samson, J. Phys. D: Appl. Phys. **37**, R179 (2004)
2. P.F. Carcia, A.D. Meinhardt, A. Suna, Appl. Phys. Lett. **47**, 178 (1985)
3. B.N. Engel, C.D. England, R. van Leeuwen, M. Nakada, C.M. Falco, J. Appl. Phys. **69**, 5643 (1991)
4. B.M. Lairson, J. Perez, C. Baldwin, IEEE Trans. Magn. **30**, 4014 (1994)
5. G. Chen, J. Appl. Phys. **87**, 6355 (2000)
6. B. Cord, O. Keitel, H. Rohrmann, K.H. Schuller, Trans. Magn. Soc. Jpn **2**, 207 (2002)
7. C. Chappert, H. Bernas, J. Ferré, V. Kottler, J.P. Jamet, Y. Chen, E. Cambril, T. Devolder, F. Rousseaux, V. Mathet, H. Launois, Science **280**, 1919 (1998)
8. T. Devolder, C. Chappert, V. Mathet, H. Bernas, Y. Chen, J.P. Jamet, J. Ferré, J. Appl. Phys. **87**, 8671 (2000)

9. J. Ferré, T. Devolder, H. Bernas, J.P. Jamet, V. Repain, M. Bauer, N. Vernier, C. Chappert, J. Phys. D: Appl. Phys. **36**, 3103 (2003)
10. T. Devolder, C. Chappert, Y. Chen, E. Cambril, H. Bernas, J.P. Jamet, J. Ferré, Appl. Phys. Lett. **74**, 3383 (1999)
11. B.D. Terris, D. Weller, L. Folks, J.E.E. Baglin, A.J. Kellock, H. Rothuizen, P. Vettiger, JAP **87**, 7004 (2000)
12. J.F. Ziegler, J.P. Biersack, U. Littmark, *The Stopping and Range of Ions in Solids* (Pergamon Press, New York, 1985)
13. M.S. Martín-González, Y. Huttel, A. Cebollada, G. Armelles, F. Briones, Surf. Sci. 2004 **571**, 63 (2004)
14. M. Sifkovits, H. Smolinski, S. Hellwig, W. Weber, J. Magn. Magn. Mater. **204**, 191 (1999)
15. S. Nakagawa, H. Yoshikawa, J. Magn. Magn. Mat. **287**, 193 (2005)
16. G.S. Bales, A. Zangwill, Phys. Rev. Lett. **63**, 692 (1989)
17. H. Sang Oh, S.Ki Joo, IEEE Trans. Magn. **32**, 4061 (1996)
18. H. Ohmori, A. Maekawa, IEEE Trans. Magn. **36**, 2384 (2000)
19. P.R.M. Johnson, M. Zheng, J. Appl. Phys. **93**, 8176 (2003)
20. I. Tagawa, A. Takeo, Y. Nakamura, J. Magn. Magn. Mat. **155**, 341 (1996)
21. Hiroku Nemoto, Yuzuru Hose, J. Appl. Phys. **97**, 10J109 (2005)
22. T. Thomson, G. Hu, B.D. Terris, Phys. Rev. Lett. **96**, 257204 (2006)
23. P.F. Carcia, W.B. Zeper, F.J.A.M. Greidanus, Mater. Res. Soc. Symp. Proc. **150**, 115 (1989)
24. T. Devolder, Phys. Rev. B **62**, 5794 (2000)
25. P.E. Kelly, K. O'Grady, P.I. Mayo, R.W. Chantrell, IEEE Trans. Magn. **25**, 3881 (1989)